analytical chemistry

Article

Cite This: Anal. Chem. 2018, 90, 988−997

pubs.acs.org/ac

Early Detection of Biofouling on Water Purification Membranes by Ambient Ionization Mass Spectrometry Imaging

Swathy Jakka Ravindran,[†] Ramesh Kumar,[†] Amitava Srimany,[†] Ligy Philip,[‡] and Thalappil Pradeep*[,†]

[†]DST Unit of Nanoscience (DST UNS) and Thematic Unit of Excellence (TUE), Department of Chemistry, Indian Institute of Technology Madras, Chennai 600036, India

[‡]EWRE Division, Department of Civil Engineering, Indian Institute of Technology Madras, Chennai 600036, India

Supporting Information

ABSTRACT: By direct analysis of water purification membranes using ambient ionization mass spectrometry, an attempt has been made to understand the molecular signatures of bacterial fouling. Membrane based purification methods are used extensively in water treatment, and a major challenge for them is biofouling. The buildup of microbes and their extracellular polymeric matrix clog the purification membranes and reduce their efficiency. To understand the early stages of bacterial fouling on water purification membranes, we have used desorption electrospray ionization mass spectrometry (DESI MS), where ion formation occurs in ambient conditions and the ionization event is surface sensitive. Biosurfactants at the air−water interface generated by microorganisms as a result of quorum sensing, influence the water−membrane interface and are important for the bacterial attachment. We show that these biosurfactants produced by bacteria can be indicator molecular species signifying initiation of biofilms on membrane surfaces, demonstrated by specific DESI MS signatures. In *Pseudomonas aeruginosa*, one of the best studied models for biofilm formation, this process is mediated by rhamnolipids forewarning bacterial fouling. Species dependent variation of such molecules can be used for the precise identification of the microorganisms, as revealed by studies on *P. aeroginosa* (ATCC 25619). The production of biosurfactants is tightly regulated at the transcriptional level by the quorum-sensing (QS) response. Thus, secretion of these extracellular molecules across the membrane surface allows rapid screening of the biofilm community. We show that, the ambient ionization mass spectrometry can detect certain toxic heavy metals present in water, using surfactant−metal complexes as analytes. We believe that such studies conducted on membranes in various input water streams will help design suitable membrane processes specific to the input streams.

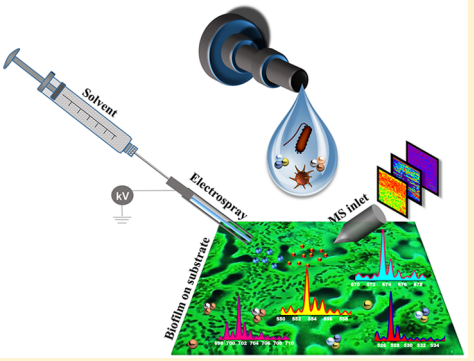

Membrane based purification has become a flourishing technology, used extensively in various industries. Membrane damage can be classified into fouling and physical and chemical damage. Fouling can be due to biofilms, particulate/colloidal matter, scaling, organics, and metals. Major impediments to the efficient operation of reverse osmosis (RO) membranes are the buildup of microbial biofilms rendering up to 31.3% of the overall volume of fouling and leads to clogging of these purification membranes.[1,2] These affected membranes are recovered back by strong alkaline treatment and disinfection, combined with procedures that consume excessive water and energy. Therefore, a successful utilization of membrane technology involves controlling membrane fouling at the earliest stage of development.

Microorganisms do not live as pure cultures of dispersed single cells but instead accumulate at the interface to form polymicrobial aggregates such as films, mats, flocs, sludges, or biofilms.[3,4] In most biofilms, the extra polymeric substances (EPS) can account for over 90% of the content with dominant fraction of the reduced-carbon reservoir serving as nutrients for the bacteria.[5,6]

The bacteria living at the same community express cell-to-cell communication known as quorum sensing (QS)[7] by secreting extra-cellular signaling molecules termed "autoinducers" that play important roles in biofilm formation.[8] It has been reported that the average concentration of these autoinducers produced is 0.33 pmol/g to 0.49 pmol/g in a well-established biofilm (3−7 days old).[9] As detection of these autoinducers at such low concentrations amidst the extensive EPS is laborious, the product of QS, namely, biosurfactants can serve as excellent indicators for biofilm initiation. These biosurfactants, generated by microorganisms at the air−water interface form a film known as conditioning film which is important for initial bacterial attachment.[10]

Surface active compounds (SACs) produced by microorganisms are ideally suited to mediate the interaction, adhesion and deadhesion, between microorganisms and surfaces.[11,12] SACs produced by different microorganisms include glycolipids and lipopeptides which are species specific.

Received: October 14, 2017
Accepted: December 6, 2017
Published: December 6, 2017

DOI: 10.1021/acs.analchem.7b04236
Anal. Chem. 2018, 90, 988−997

Interestingly, these surface-active extracellular lipids apart from surface activity have been proposed to act in initial microcolony formation, facilitating bacterial migration and the formation of mushroom-shaped structures, preventing colonization of channels and playing a part in biofilm dispersion.[13]

The Gram-negative bacterium, *Pseudomonas aeruginosa* is one of the best studied models for biofilm formation and has been chosen for studying these two social phenomena independently, namely, quorum sensing and biofilm formation.[14] *P. aeruginosa* is ubiquitous and an opportunistic pathogen causing serious infections.[15] This bacterium was shown to produce glycolipidic biosurfactants named rhamnolipids, which are amphiphilic molecules composed of a hydrophobic fatty acid and a hydrophilic portion composed of rhamnose moieties.[16] Liquid chromatography coupled with mass spectrometry (LC−MS) allowed the detection of more than 28 different rhamnolipid congeners with alkyl chains varying from C8 to C12.[17] The transcriptional regulation of rhamnolipids occurs in a cell density-dependent manner through QS.[18,19] Interestingly, rhamnolipids have been found in the EPS matrix of *P. aeruginosa* playing vital roles in biofilm cohesion.[20,21]

Among the complex EPS, *Alginate* is a distinct exopolysaccharide that contributes to biofilm development and architecture. Polyhydroxyalkanoate (PHA) is a versatile class of biopolyesters accumulated by many bacteria as carbon storage compounds. 4-Hydroxy-2-alkylquinolines (HAQs) are a class of signaling molecules produced by various types of bacteria and are involved in quorum sensing. The rhamnolipid biosynthetic pathway shows metabolic links with all the three of these bacterial products such as alginate, PHA, HAQs and also with lipopolysaccharides.[22]

Understanding biofouling on membranes at a molecular level has been a desired objective in water purification. Because of the diversity in input water streams, species specific detection of bacteria at purification membranes, especially with limited sample preparation, under ambient conditions can lead to new insights into the bacterial growth and contribute to appropriate remediation.[23] A mature biofilm affords the bacterial community with protection from a wide range of intensive antimicrobial treatments due to which recovering the expensive water purification membranes is a challenge.[24] Biofilms secrete a matrix of EPSs which obstruct the overall water purification process leading to choking of membranes, decline in permeate water flux, decrease in salt rejection, and thus elevating the osmotic pressure near the membrane surface.[25] These result in increased operation and maintenance costs and ultimately the membrane life is shortened.[26] Hence, good monitoring systems are necessary for the development and optimization of efficient antibiofouling strategies. Monitoring techniques should be able to detect the composition, stages, and kinetics of the growth of the biofilm. Information on biofouling should be acquired *in situ*, in real time, nondestructively, and accurately before significant irreversible loss occurs.[25]

Desorption electrospray ionization mass spectrometry (DESI MS) is a label free, ambient ionization technique which is used for surface sampling, high-throughput analysis, and chemical imaging of surfaces.[27] Mass spectrometry imaging (MSI) allows the two-dimensional visualization of the distribution of trace metals, metabolites, surface lipids, peptides, and proteins directly from biological samples without the need for chemical tagging or antibodies.[28] These features make MSI a useful tool for visualizing small molecules, which can otherwise be difficult to reliably label and distinguish from structurally similar compounds.[29,30] Thus, DESI MS is one of the fastest and easiest methods of direct analysis of surfaces, and its adaptation to membrane fouling can provide molecular information pertaining to initiation of bacterial biofilms.[31] As molecular signatures are species specific, immediate identification of the causative microorganism is possible. As remediation is also molecular in nature, a DESI MS analysis provides a study of both the problem and the solution simultaneously.[32] Biosurfactants being a direct indication of microbial fouling, they form the analyte of interest in this study. Moreover, these microbial surfactants have several desirable properties and is a favorable case for DESI analysis; because, first, they are excreted in and around the bacterial consortia and so are highly available; second, they are powerful surfactants and reduce the surface tension of water, facilitating secondary droplet formation in DESI; third, their relatively high molecular weights mean that there is minimal interference from other molecules outside or within the biofilm; and fourth, their polar functional groups allow ready ionization in both positive and negative ion modes of DESI MS.[33]

Apart from quorum sensing and biofilm formation, the rhamnolipids produced by *P. aeruginosa* sequester heavy metals (e.g., Cd^{2+}, Pb^{2+}) and degrade hazardous organic contaminants. The complex class of biosurfactants transform these heavy metals to less toxic forms or decrease their mobility through reactions like oxidation, reduction, precipitation, or other transformations.[34] Different approaches have been used for the determination of trace levels of heavy metals in water. Mass spectrometric detection of these heavy metals include intricate procedures like preconcentration for the determination of trace quantities ($\mu g\ L^{-1}$) in water samples, dosed injection of liquid samples (2.5−20.0 μL) into a vacuum chamber, extraction of salts containing target components, etc. Whereas, the rhamnolipid−metal adducts formed on the biofilms of membrane surfaces can be detected directly by DESI MS, at ambient atmosphere with no sample pretreatment.

In the following, we present a study of the evolution of bacterial fouling at water purification membranes. Our study involves time dependent DESI MS imaging of the substrate undergoing continuous exposure to input water stream composed of different organisms separately as well as collectively. Bacterial adhesion and subsequent biofilm formation are visualized here. DESI MS analyses were performed without sample preparation and were carried out in the presence of common interfering biological matrixes, such as nutrient broth, extracellular proteins, lipids, cellular fractions, and other EPS constituents. We show that biosurfactants produced by bacteria can be indicator molecules with which biofilm formation can be foreseen and monitored effectively. Moreover, the complexation of rhamnolipids with heavy metals can be made useful as a method of ultrasensitive detection. The rhamnolipids secreted on membranes as a result of biofilm formation when exposed to water contaminated with heavy metals can form unique complexes. DESI being a surface desorption ionization process, it also enables the detection of metal−rhamnolipid complexes from a biofilm surface. This demonstrates a way of simultaneous detection of contamination in input water streams.

EXPERIMENTAL SECTION

Culturing Bacterial Strains. *Pseudomonas aeruginosa* (ATCC 25619) was a gift from Dr. M. Krishnaraj (ABTRI Biotech Pvt. Ltd., Chennai). *Bacillus subtilis* (ATCC 21331)

DOI: 10.1021/acs.analchem.7b04236
Anal. Chem. 2018, 90, 988−997

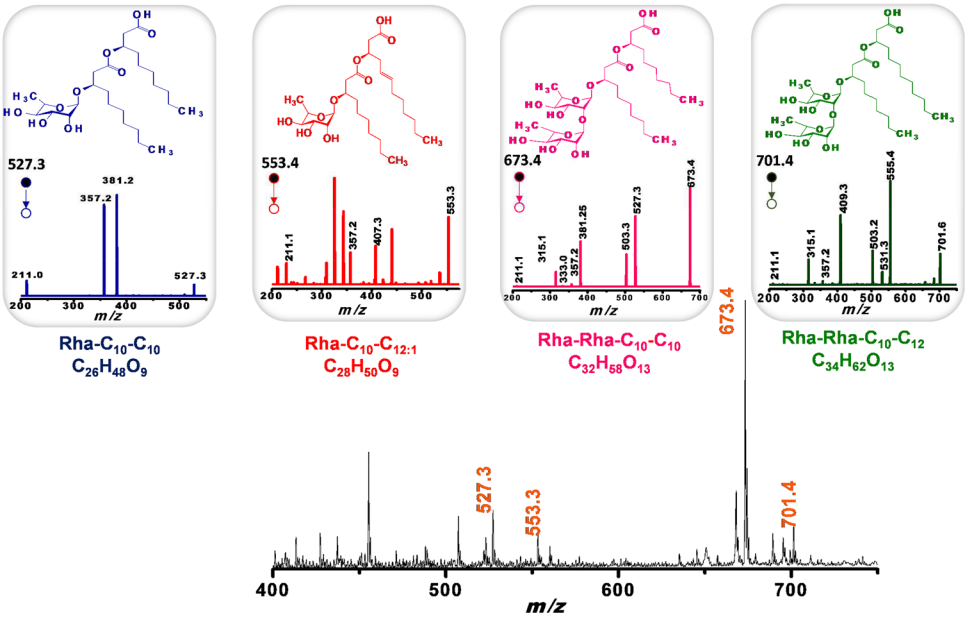

Figure 1. Positive mode DESI mass spectrum of Gram-negative bacterial biofilm recorded from nylon membranes and corresponding MS/MS product ion spectra. Mass spectrum of *P. aeruginosa* (ATCC 25619) biofilm observed in positive ion mode showing peaks at *m/z* 527.3, 553.4, 673.4, and 701.4 (bottom). The specified peaks represent the sodium adducts of rhamnolipids secreted by *P. aeruginosa* at initial stages (24 h) of adsorption on the surfaces. Fragmentation patterns of mono- and dirhamnolipids secreted by the organism during the biofilm growth and their deduced structure are shown (top). The peak at *m/z* 553.4 corresponds to both Rha-C10-C12:1/Rha-C12:1-C10 and that at *m/z* 701.4 corresponds to both Rha-Rha-C10-C12/Rha-Rha-C12-C10.

was a gift from Prof. S. Gummadi (Department of Biotechnology, IITM). A single colony of the bacteria from Luria–Bertani (LB) agar was inoculated into LB broth. This overnight culture was rediluted in LB broth enriched with glucose carbon source (150 μL of 1.2 M glucose per 6 mL of culture, sterilized using 0.2 μm filter)[35] and were allowed to grow at 37 °C to late exponential phase with an optical density (600 nm) of 1. This was used as inoculum for the biofouling experiments. Growth of biofilms in static and continuous flow units is described in Supporting Information 1.

INSTRUMENTATION

Mass Spectrometry and Imaging. *Analysis of Biofilm Extracts: ESI MS and MS/MS.* Comparative ESI MS data was recorded with a commercial Thermo Scientific LTQ (San Jose, CA) linear ion trap mass spectrometer. Mass spectra were collected at spray voltage, 5 kV; capillary temperature, 250 °C; sheath gas (N_2) flow rate, 20 units; sample flow rate, 5 μL/min. All the ESI mass spectra shown are an average of approximately 50 consecutive scans. Extraction of biofilm is explained in the Supporting Information 2.

Direct DESI MS of Membranes. DESI analysis were performed with a Thermo Scientific LTQ (San Jose, CA) linear ion trap mass spectrometer equipped with an automated DESI source of Prosolia (Indianapolis, IN). Biofilm covered membranes were air-dried and cut in the desired dimension and fastened onto the glass plate of the DESI stage. The spray solvent used in the positive mode was 0.1% acidified methanol–water (50:50) and in negative mode was methanol.[36] Mass spectra were acquired in both the modes in the mass range of *m/z* 50–2000 under the following optimized conditions: sample distance 5 mm, spray voltage ±5 kV, capillary temperature 250 °C, capillary voltage ±45 V and tube lens voltage ±100 V, nitrogen gas pressure 120 psi, and solvent flow rate 3 μL/min. All DESI mass spectra presented correspond to an average of 30 scans.

Tandem mass spectrometry was performed with collision-induced dissociation (CID) with isolation width, 1 *m/z*; normalized collision energy, 25–35 (manufacturer's unit); activation Q, 0.250 (manufacturer's unit); and activation time, 30 ms.

Mass Spectrometry Imaging. The thickness of these biofilms were in the range of 3 μm which did not alter the signal intensity. By limiting the solvent flow rate to 3 μL/min, efforts were taken to prevent smearing of the analyte. To avoid experimental artifacts, all the substrates in this study were grown in the same culture condition and analyzed continuously one after another using a fixed sample stage and spray parameters.

The membranes were scanned using a 2D-moving stage over the range of *m/z* 50–2000. A spatial resolution (pixel size) of 250 μm × 250 μm was used and other parameters were same as in DESI MS. The Firefly program allowed the conversion of the raw files acquired by XCalibur 2.0 into a format compatible with the BioMap (freeware, http://www.maldi-msi.org) software to visualize the images. The individual spectrum acquired were assembled into a spatially accurate two-dimensional ion image using the BioMap software.

MS Analysis of Rhamnolipid–Metal Complexes. For a 1:1 ligand–metal ratio, 1 mM rhamnolipid solution with 1 mM $Cd(NO_3)_2$ or $Pb(NO_3)_2$ were mixed in water and pH-adjusted to 5.0 with HCl. Solutions were diluted 1/10 in acidified methanol–water (1:1) for ESI MS and were directly spotted on Whattman filter paper for DESI MS analysis. For MS/MS analysis, normalized collision energy of 25–35 (manufacturer's unit) was used.

Scanning Electron Microscopy Imaging. Substrates exposed to biofilm growth were rinsed twice with sterile saline and placed in 5% glutaraldehyde (fixative) for 30 min at 25 °C.

DOI: 10.1021/acs.analchem.7b04236
Anal. Chem. 2018, 90, 988–997

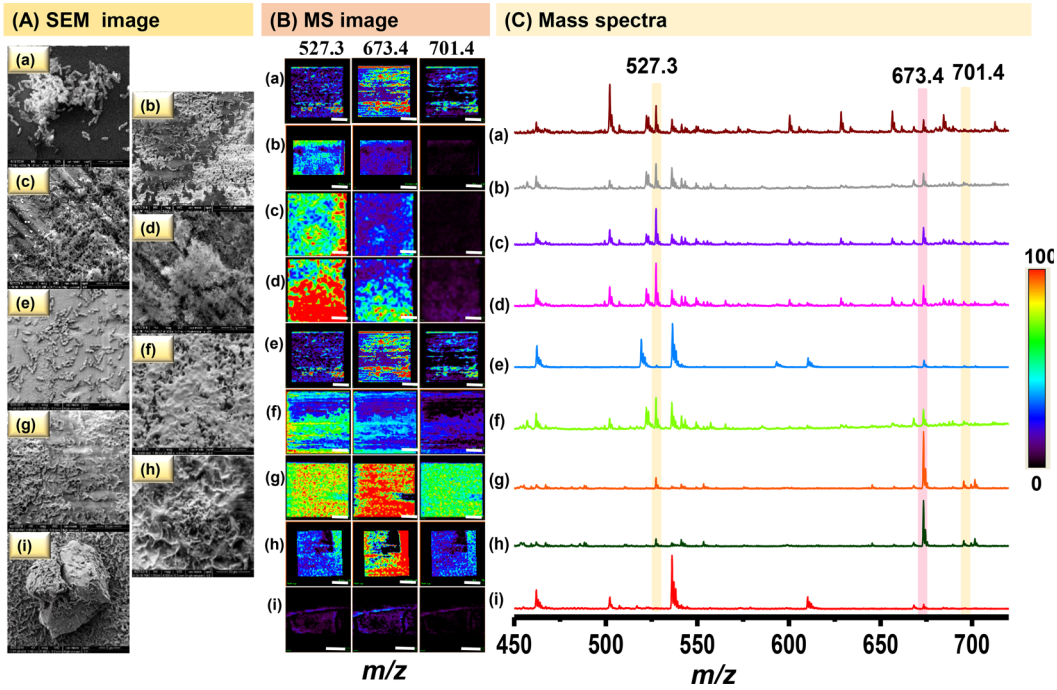

Figure 2. (A) SEM images, (B) positive mode DESI MS images, and (C) DESI mass spectra from various substrates. The substrates are (a) glass (b) polypropylene, (c) polyvinyl chloride, (d) polysulfone, (e) RO membrane, (f) nylon membrane, (g) aluminum, (h) copper, and (i) a water purification composite. Sodium adducts of different rhamnolipids are seen at *m/z* 527.3, 673.4, and 701.4, the spatial profiles of which are shown in part B. The scale bar in DESI MS images corresponds to 5 mm and are same in all the images. DESI MS images are color coded, and the color code is shown on the right.

Substrates were then dehydrated using graded series of ethanol (from 10% to 100%) for 10 min each and air-dried. The surfaces were metallized by gold sputtering and examined using a scanning electron microscope (FEI Quanta 200).

RO Membrane, Crossflow Test Unit, and Biofouling Protocol. A laboratory-scale test unit was used for the crossflow study. A detailed description of the experimental setup is given in Supporting Information 3. Five sets of individual experiments were conducted at 1, 2, 3, 4, and 5 days of operation. Biofilm grown samples were collected as such, stored, and analyzed using DESI MS to track the molecular signals at different stages of the biofilm.

RESULTS AND DISCUSSION

Biosurfactants generated by microorganisms at the interface influence the interfacial tension and thus aid initial microcolony formation. An alternative ecological role for these surfactants relates to their toxicity against a variety of microorganisms, which might confer a competitive advantage in niche colonization. *P. aeruginosa* being a notoriously successful and ubiquitous bacterium establishes its dominance over other bacterial populations in the habitat using rhamnolipids,[37] while this activity is exhibited by surfactin in *Bacillus sp.* Therefore, species specific biosurfactants were chosen as analytes of interest. *Pseudomonas* and *Bacillus* are some of the best studied models for biofilm formation. Because of their metal sequestration property, the surfactant−metal adducts were also demonstrated as analytes for heavy metals detection in water.

DESI Mass Spectra: Signals of Biofilm Initiation from Water Purification Membranes. The average positive ion spectrum and corresponding MS/MS product ion spectra acquired from the membranes exposed to *P. aeruginosa* is shown in Figure 1. The positive ion data sets were analyzed for species specific surfactants. These surfactants produced by *P. aeruginosa* signifying biofilm formation were identified as rhamnolipids. The vast majority of *P. aeruginosa* strains produce a mixture of mono- and dirhamnolipids. Rhamnolipids are typically constituted of a dimer of 3-hydroxy fatty acids linked through a *β*-glycosidic bond to a mono- or dirhamnose moiety. In liquid culture and under usual growth conditions, the two most abundant rhamnolipids observed are L-rhamnosyl-3-hydroxydecanoyl-3-hydroxydecanoate (Rha-C10-C10, MW 504 g/mol), a monorhamnolipid, and L-rhamnosyl-rhamnosyl-3-hydroxydecanoyl-3-hydroxydecanoate (Rha-Rha-C10-C10, MW 650 g/mol), a dirhamnolipid.[25] These two abundant rhamnolipids were observed as sodium adducts at *m/z* 527.3 and *m/z* 673.4, respectively. The peak at *m/z* 553.4 is accompanied by a peak at *m/z* 555.4, corresponding to the Na^+ adduct of the rhamnolipid congener with MW 532. The peak at *m/z* 553.4 corresponds to the Na^+ adduct of unsaturated rhamnolipid congeners with MW 530. The fact that many congeners are produced indicates that enzymes involved in fatty acid biosynthesis are not highly specific for the *β*-hydroxydecanoyl moiety. The mass profiles obtained directly from unperturbed RO membranes were confirmed as mono- and dirhamnolipids using MS/MS. The fragmentation pattern was in agreement with previously published fragmentation analysis[28,29] and that of commercial standards (Figure S1).

Similarly, the surfactant produced by *B. subtilis* was detected as shown in Figure S2. The dominant peak at *m/z* 1059.2 was identified as the sodiated cation of surfactin (C15), a cyclic lipoheptapeptide ($C_{13}H_{27}HCOCH_2CO$-Glu-Leu-D-Leu-Val-Asp-D-Leu-Leu) containing a *β*-hydroxy C_{15} fatty acid with a calculated monoisotopic MW of 1035.7. Lower homologues due to the known C14 and C13 surfactins occur at *m/z* 1045.1

DOI: 10.1021/acs.analchem.7b04236
Anal. Chem. 2018, 90, 988−997

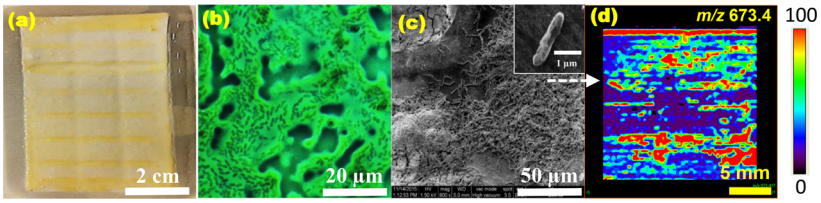

Figure 3. Comparative visualization of biofilms. (a) Photograph of RO membrane after biofilm growth (6 days). Marks on the membrane are due to the spacers used. (b) Dark field microscopic image of the biofilm (1 day growth). (c) SEM image of the biofilm (1 day growth). (d) Positive mode DESI MS image of the ion m/z 673.4 (Rha-Rha-C10-C10 expressed on the biofilm after 1 day growth). DESI MS image is color coded, and the color code is shown on the right.

and 1031.1, respectively. Shown in the left inset is the MS/MS product ion spectrum of [surfactin (C15) + Na]$^+$. The fragment ion observed at m/z 945.7 corresponds to the elimination of a Leu residue, that at m/z 832.7 is due to the loss of two such residues, and that at m/z 814.6 is due to the further elimination of a molecule of water.[29]

The negative ion DESI mass spectra obtained from *P. aeruginosa* and *B. subtilis* grown on purification membranes under the same experimental conditions are shown in Figure S3. The two most abundant rhamnolipids shown in Figure S3a are Rha-C10-C10 (MW 504 g/mol) and Rha-Rha-C10-C10 (MW 650 g/mol), observed as m/z 503.5 and m/z 649.6, respectively. The other congeners present were detected as m/z 529.3, 531.3, and 677.4. In the case of *B. subtilis* shown in Figure S3b, the intact lipopeptide is the dominant species. The singly charged surfactin(C15) [surfactin(C15) − H]$^-$ is the dominant ion observed at m/z 1035.0. The spectrum shows the lower homologue surfactin (C14) at m/z 1021.0 and surfactin (C13) at m/z 1007.0. The ion m/z 1057.0 is having the molecular formula [M + Na − 2H]$^-$.

Analysis of Biofilm by DESI MS Imaging (DESI MSI). A signature application of DESI MS is ambient mass spectrometric imaging used to map the spatial distribution of exogenous or endogenous chemicals. Because of the ambient nature and softness of DESI ionization, the unmodified native sample can be imaged without sample pretreatment, thus avoiding any possibility of contamination with exogenous compounds. DESI being a surface desorption ionization process, it enables imaging of analytes from a given surface by directing the spray to small segments, systematically. So a challenge in DESI MS is to acquire consistent mass profiles from different sample surfaces. The reported substrates for DESI MS include polytetrafluoroethylene (PTFE), TLC-plates, porous silicon, alumina, Whattman filter paper, and nylon.[38−41]

To demonstrate the efficiency of this technique, we present biofilm detection from different surfaces like polymers, water purification membranes, metals, and water purification materials. Figure 2 shows typical DESI MS profiles with corresponding single ion MS images and SEM where the spatial distribution of both mono- and dirhamnolipids are expressed on different substrates. Examination of the positive mode single m/z images revealed the localization of the dirhamnolipid, Rha-Rha-C10-C10 at m/z 673.4, expressed comparatively at a higher concentration than m/z 701.4 and m/z 527.3. Reasons for the difference in the concentration of mono and dirhamnolipid secretion in different surfaces are unclear from the available literature. The substrates demonstrated are (a) glass, (b) polypropylene, (c) polyvinyl chloride, (d) polysulfone, (e) RO membrane, (f) nylon membrane, (g) aluminum, (h) copper, and (i) a water purification composite. The study was aimed at illustrating the application of DESI MS in the detection of molecular markers of biofilm on multiple substrates and it does not provide a comparison of chemical images across substrates which are unrelated to one another. Irregularities on surfaces promote bacterial adhesion and biofilm deposition whereas the ultrasmooth surfaces do not favor it. As surfaces like glass and polypropylene were ultrasmooth surfaces (as seen in SEM), it is anticipated that the biofilm growth was limited to the given growth period and hence reflected in poor DESI signals. Whereas, the surfaces like polyvinyl chloride, polysulfone, RO membrane, nylon membrane, aluminum, copper, and water purification composite were found to be microscopically rough. Therefore, expression of biofilm and the corresponding DESI signals were enhanced in Figure 2c,d,f−h. It should be noted that RO-membrane (e) and water purification composite (i) used in Figure 2 serve as negative controls and are from commercial products which were already protected with antimicrobial agents. This prevented the expression of biofilms at the given growth period depicted by reduced signal intensity in DESI mass spectra.

Observing Various Stages of the Biofilm. A comparative visualization of biofilms by digital, optical dark field microscopic, electron microscopic, and mass spectrometric imaging are shown in Figure 3, which demonstrates the molecular distribution to understand the age of the biofilms. Figure 3a represents the digital photograph of a reverse osmosis membrane after 5 days of growth, as described in the Experimental Section. The membrane shows a slimy layer of biofilm grown at the bacteria accumulated regions. Figure 3b is a dark field image of the development of the biofilm, and Figure 3c is the SEM image of the same and the inset shows the morphology of a single bacterium. Figure 3d is the mass spectrometric image collected using DESI MSI. In the process of studying membrane fouling, it is also necessary to understand the region exposed to excessive fouling revealed by molecular imaging. Such imaging would be necessary in order to study the variation in the concentration of the molecular species across the membranes spatiotemporally, which are not observable from single spot spectra. For example, since the ion m/z 673.3 (in Figure 3) is not uniformly distributed across the surface in all the samples, it could be missed if not imaged across the membrane. Analysis of *B. subtilis* biofilm (surfactin) is shown in Figure S4. Figure S4a represents the DESI MS spectrum, and Figure S4b shows single ion DESI MSI collected from the membrane surface where the spatial distribution of surfactin is revealed.

The evolution of biofilm with time is proportionate to the increase in concentration of rhamnolipids within the matrix. Mass profiles of the rhamnolipids produced within and on the biofilm of *P. aeruginosa* collected on five consecutive days (within 4 h and after 12, 24, 48, 72, 96, and 120 h) were

DOI: 10.1021/acs.analchem.7b04236
Anal. Chem. 2018, 90, 988−997

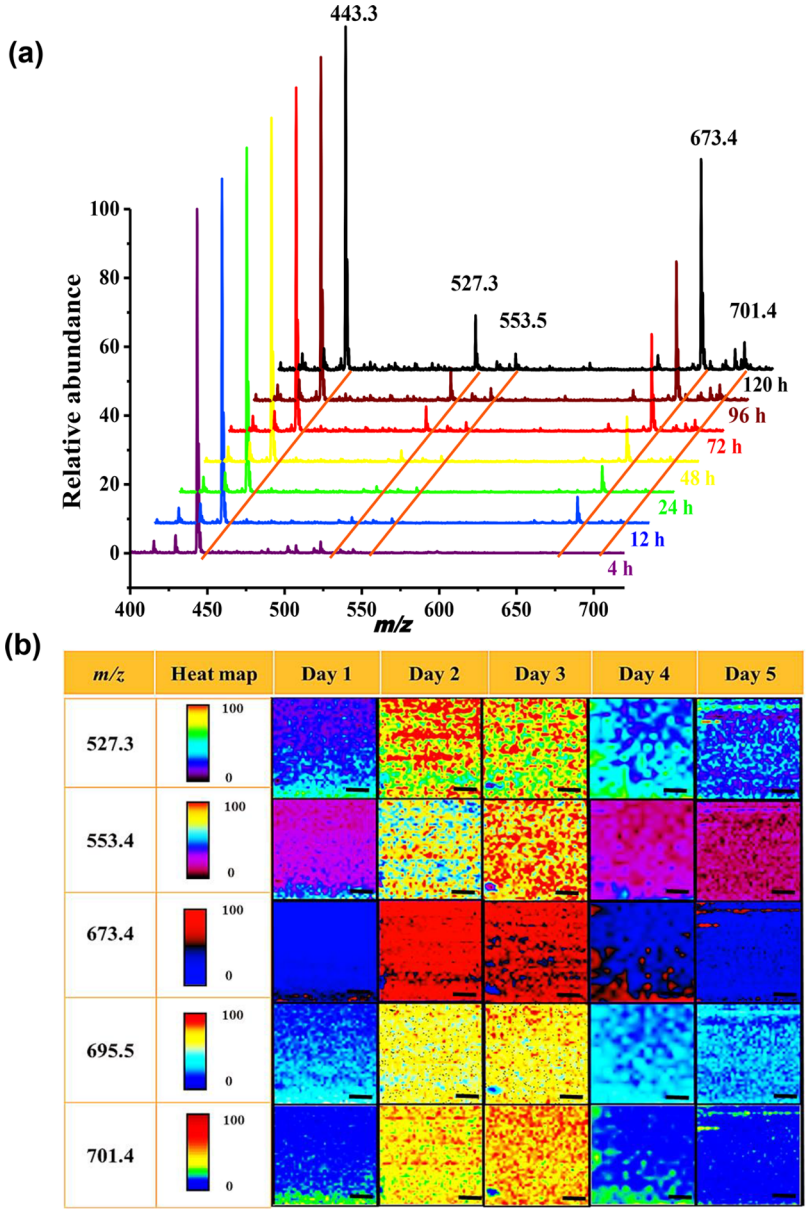

Figure 4. Mass spectrometric representation of progression in biofilm development with time. (a) Electrospray ionization mass spectra (ESI MS) corresponds to rhamnolipids of biofilms collected within 4 h, after 12, 24, 48, 72, 96, and 120 h (up to 5 days). The m/z 443.3 ion is an internal standard (Rhodamine 6G) used in a fixed concentration in all the samples for normalizing every individual spectrum. (b) Individual DESI mass spectral image scan collected from the RO membrane cross-flow test unit after 24, 48, 72, 96, and 120 h (up to 5 days). The scale bar corresponds to 5 mm and is the same in all the images. The images are normalized across the rows, and the corresponding color codes are shown under the heat map column.

analyzed using ESI and DESI MS as shown in Figure 4. A quantitative comparison of rhamnolipids secreted at different ages of the biofilm was performed by analyzing the signal intensity of the signature analyte from the acquired mass spectra. The peak at m/z 443.3 is an internal standard (Rhodamine 6G) used at a standard concentration in all the samples for normalizing individual spectra. In a typical ESI MS experiment, the biofilm was extracted as described in the Experimental Section. Representative positive ion ESI mass spectra obtained for each concentration exhibiting modest linearity with time are shown in Figure 4a. A peak area vs time plot is shown in Figure S5 showing modest linearity. A lab scale RO membrane cross-flow test unit with 5 sets of individual experiments were conducted for 1−5 days of operation and the membranes were collected and biofilms were imaged using DESI MS (Figure 4b). Scanned image profiles are expressed as heat maps. Different color maps for each of the lipids is given to emphasize that the comparison is to be made across the rows and not between the columns. The cross-flow test unit used for this study is represented schematically in Figure S6a. The fall in permeation level and the drop in flux are depicted in Figure S6b,c, respectively. The biofilm formation in *Pseudomonas aeruginosa* proceeds sequentially, and five stages have been proposed. Stage one is generally identified by a transient association with the surface, followed by robust adhesion in stage two. Stages three and four involve the aggregation of cells into microcolonies and subsequent growth and maturation. Biofilm structures form three-dimensional growth at this stage,

DOI: 10.1021/acs.analchem.7b04236
Anal. Chem. 2018, 90, 988−997

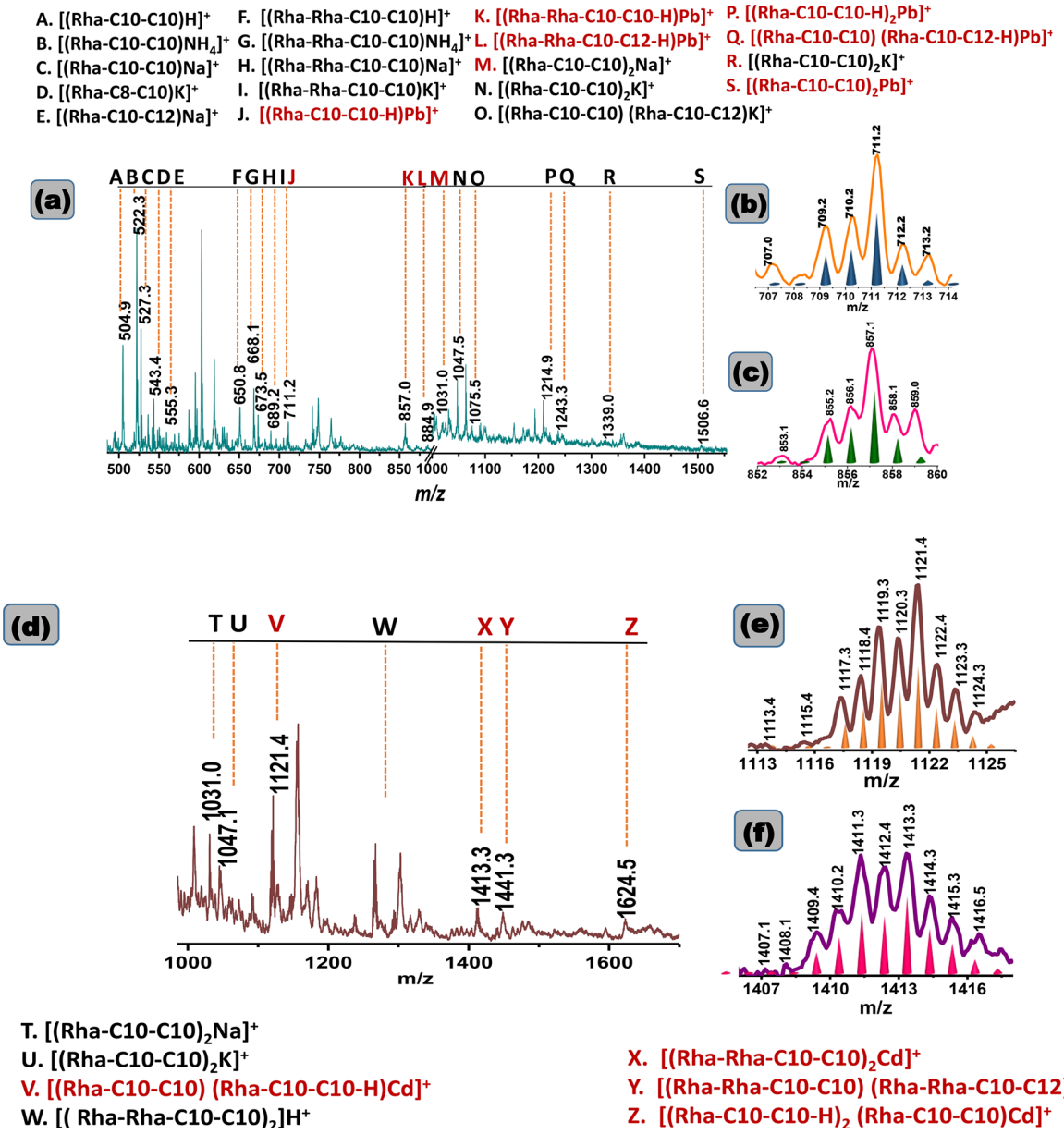

Figure 5. (a) Positive mode DESI mass spectrum of rhamnolipid−metal adducts of RL−Pb^{2+} species, (b,c) isotopic distribution of m/z 857.0 and m/z 711.1 including simulated MS spectra, (d) positive mode DESI mass spectrum of rhamnolipid−metal adducts of RL−Cd^{2+} species and (e,f) isotopic distribution of m/z 1121.4 and m/z 1413.3 including simulated MS spectra.

forming a protective cover. Stage five is characterized by a return to transient motility where biofilm cells are sloughed or shed.[42] These stages are represented directly by the exposure of rhamnolipids to the surface, shown using DESI MSI. The image scan shows the decreased distribution of lipids in the initial sample (day 1), whereas successive samples (days 2 and 3) showed progressive lipid secretion on the membranes. DESI MS being a surface analysis technique, the succeeding stages of cell aggregation and three-dimensional growth masks the lipids within the EPS leading to decreased signal intensity from the outer surface. Because of this surface sensitivity, it is impractical by DESI MS to quantitate the overall lipids secreted within the entire biomass at any specified time and thus serves only as a qualitative measure. In order to quantify, liquid extraction procedures will be required. On scouring off the EPS cover manually, the rhamnolipids beneath the layer was exposed and thus corresponding signals started to appear (Figure S7). The signal intensities of rhamnolipids were specifically enhanced in the scrapped regions than other signals that emerged from the sample surface whose intensity remained the same. This proved that the process of scraping off the surface revealed the rhamnolipids trapped within.

Species Specific Identification. In some instances, biofilms are populated by a single species, whereas in others, the inhabitants are comprised of a diverse microbial array. Multispecies biofilms can form stable micro consortia, develop physiochemical gradients, and undergo intense cell−cell communication, and these consortia therefore represent highly competitive environments. In order to test the sensitivity of this analysis methodology in such diverse conditions, we assayed single- and dual-species bacterial biofilms (Figure S8). DESI signals were collected from a mixed biofilm culture of two dominant species in the environment, namely, *Pseudomonas* and *Bacillus* where the spectrum revealed peaks representing both

DOI: 10.1021/acs.analchem.7b04236
Anal. Chem. 2018, 90, 988−997

the organisms. Features of both rhamnolipids as well as surfactin was observed. Thus, this proves that the method can be used over an assorted biofilm environment to identify the heterogeneity of the biofilm community.

Heavy Metal Detection from RL−Metal Complexes. Parent ion masses observed for rhamnolipid (RL) and metal complexes, RL−Pb^{2+} and RL−Cd^{2+}, are shown in Table S1, and their corresponding mass spectra are shown in Figure 5a,d. Several metal complexes are recognized in MS by the unique spectral patterns due to their distinct isotopic distributions. For Pb^{2+}, this distribution has ^{204}Pb (1.4%), ^{206}Pb (24.1%), ^{207}Pb (22.1%), and ^{208}Pb (52.4%) for an average atomic mass of 207.2. Isotopic patterns of monoRL−Pb adduct at m/z 711.1 and diRL−Pb adduct at m/z 856.9 are similar to their particular theoretical patterns, shown in Figure 5b,c, respectively. It should be noted that the standard used was a sample of 90% pure rhamnolipid mixture. The differences in other adducts might be due to the bacterial cultures and purification conditions used by the manufacturers.

The characteristic fragmentation patterns of these adducts were observed by MS/MS, shown in Figure S9. The weak fragment as m/z 606.9 in Figure S9a corresponds to a loss of m/z 104.1 from an inner rhamnosyl fragment. The most abundant peak with m/z 565.0 corresponds to a loss of m/z 146.1 (complete rhamnose sugar). No fragments corresponding to a rhamnosyl moiety−Pb^{2+} have been observed. These results suggest that Pb^{2+} is associated with the fatty acid end of the monoRL. In Figure S9b, the fragmentation of diRL−Pb peak (m/z 856.9) results primarily in the loss of one and two rhamnosyl groups from the diRL resulting in peaks at m/z 709.9 and m/z 564.9, respectively, and this supports the suggestion that Pb^{2+} binds to the fatty acid tails.

The unique isotopic distribution of cadmium is a useful marker. It includes ^{106}Cd (1.25%), ^{108}Cd (0.89%), ^{110}Cd (12.49%), ^{111}Cd (12.80%), ^{112}Cd (24.13%), ^{113}Cd (12.22%), ^{114}Cd (28.73%), and ^{115}Cd (7.49%). The Cd-containing ion observed at m/z 1121.2 corresponds to a monoRL dimer with one Cd^{2+} in the form of $[(\text{Rha-C10-C10})\ (\text{Rha-C10-C10} - \text{H})\text{Cd}]^+$ and that at m/z 1413.1 corresponds to $[(\text{Rha-Rha-C10-C10})_2\text{Cd}]^+$. The isotopic Cd^{2+} complexes associated with m/z 1121.2 and m/z 1143.3 ions are shown in Figure 5e,f, respectively, and their identity is confirmed by MS simulation (inset). Fragmentation of the ion at m/z 1121.2 (Figure S9c) shows the loss of the first (m/z 974.0) and second (m/z 828.1) rhamnose sugars. The fragment at m/z 656.7 represents further loss of one C10 lipid tail from the m/z 828.8 species. Since the observed fragment ions retain Cd^{2+}, it may be concluded that Cd^{2+} is complexed by the resulting lipid tail.[43]

The production of several virulence-associated traits, including rhamnolipids, are a result of quorum signaling regulated at the transcriptional level.[44] The production of important structural compounds involved in biofilm architecture like alginate, PHA, etc., have biosynthetic steps common with these surface-active exoproducts like rhamnolipids, thus indicating the initiation of biofilms.[17,45]

DESI imaging enables visualization of molecular distributions in complex environments like biofilms. Amidst the multifaceted nature of the self-produced matrix, encompassing hydrated EPS, mainly polysaccharides, proteins, nucleic acids, and lipids, a direct identification of the molecule of interest in an ambient environment is possible without sample preparation. The approach was validated with *P. aeruginosa* in order to visualize the chemical features associated with growth and cellular signaling. While several genus, species, and sub species of bacteria are involved in biofilm formation, *P. aeruginosa* is noted to be a notoriously successful and ubiquitous bacterium. This is because of their dominance over other species empowered by the surface-active molecules possessing toxicity against various species.[46] Even when multispecies biofilms can form stable microconsortia, dominance of a few pervasive and ubiquitous bacteria like *Pseudomonas* can be chosen as indicator organisms to track biofilm initiation. While the production of rhamnolipids is characteristic of *P. aeruginosa*, some isolates of the nonpathogenic pseudomonads, *P. putida* and *P. chlororaphis* as well as the pathogen, *Burkholderia pseudomallei* were also shown to produce a variety of rhamnolipids.[47,48] Although mass profiles of rhamnolipids varied between 28 different congeners, the presence of the two most abundant rhamnolipids, MW 504 and MW 650, are found to be common to confirm the biofilm community.

While mass spectrometric detection of heavy metals involve intense procedures, their complexation with rhamnolipids made the detection simple. A simultaneous detection of biofilms by the presence of rhamnolipids and the detection of heavy metals by the presence of rhamnolipid−metal complexes on unmodified membrane surfaces in ambient atmosphere was possible using DESI MS.

CONCLUSION

In this study, we have used a spatiotemporal chemical imaging approach at ambient atmosphere wherein no sample preparation was required to target bacterial exoproducts amidst the intricate biofilm matrix. We demonstrated that initiation of biofouling on RO membranes can be understood using DESI MS at a species specific level. High-quality mass spectra were obtained in both positive and negative ion modes, when the bacterial biofilms growing on membrane surfaces were subjected to DESI MS studies.

This combination of mass spectrometry with imaging conveys numerous advantages in an experiment, including (1) illustration of species specific biofilm initiation from a chemical map rather than an unperceptive optical image, (2) classification of the heterogeneity of the biofilms by chemical images, (3) adaption to nonspecific assorted substrates unlike microscopy, and (4) capability of DESI MS/MS molecular characterization.

The detection of biofilms at initial stages can reduce the burden of intensive treatments for the removal of matured bacterial matrix which gets strengthened mechanically by extracellular polymeric substances. Detection at earlier stages can thus extend the life span of expensive membranes. The RO membranes were unperturbed after the experiment, which is understandable due to the small volume of the solvent used and the exposure of only a small fraction of the surface to the solvent. We illustrate that both single- and multiple-species biofilms can be analyzed by this technique. This study demonstrates the capability of DESI MS for *in vivo* biofilm characterization, differentiation of Gram-positive and Gram-negative bacterial biofouling, and concurrent heavy metal analysis. The secreted glycolipids and lipopeptides are highly species-specific and have been previously used as the main chemical entities in differentiation of different microorganisms. As analysis is based on rhamnolipids, subspecies differentiation may be possible in the future. This chemical specificity and identification of organisms involved in the biofilm formation can help in deciding the remediation strategies. Most of these

DOI: 10.1021/acs.analchem.7b04236
Anal. Chem. 2018, 90, 988−997

lipids are used for bioremediation, as they complex with the heavy metals in the environment. This complex formation makes the detection of metals possible using DESI MS. We are aware that several experiments will be necessary to improve the application of DESI in simultaneous detection of heavy metals, hydrocarbons, pesticides, and other contaminants present in fresh water. *In vivo* nature of these experiments makes the analysis instantaneous and thus help advance the subject of rapid detection of hazardous bioagents and inorganic contaminants in drinking water. With DESI being a surface ionization process, it is impractical currently to quantitate the total analyte present and may be better employed as a qualitative measure.

■ ASSOCIATED CONTENT

Supporting Information

The Supporting Information is available free of charge on the ACS Publications website at DOI: 10.1021/acs.analchem.7b04236.

MS/MS product ion spectra of the rhamnolipids, negative mode DESI MS of biofilms, MSI of a *B. subtilis* biofilm, and cross-flow test unit (PDF)

■ AUTHOR INFORMATION

Corresponding Author

*E-mail: pradeep@iitm.ac.in. Fax: +91-44-2257-0545.

ORCID

Swathy Jakka Ravindran: 0000-0002-7882-7871

Thalappil Pradeep: 0000-0003-3174-534X

Notes

The authors declare no competing financial interest.

■ ACKNOWLEDGMENTS

We thank Anil Kumar Avula for providing water purification materials. We thank Mr. Sundar Raj for technical support in SEM analysis. We thank SAIF, IITM for providing the gold sputtering facility. We thank the Department of Science and Technology (Government of India) for constantly supporting our research on nanomaterials.

■ REFERENCES

(1) Herzberg, M.; Elimelech, M. *ISME J.* **2008**, *2*, 180−194.
(2) Vrijenhoek, E. M.; Hong, S.; Elimelech, M. *J. Membr. Sci.* **2001**, *188*, 115−128.
(3) Xavier, J. B.; Foster, K. R. *Proc. Natl. Acad. Sci. U. S. A.* **2007**, *104*, 876−881.
(4) Wingender, J.; Neu, T. R.; Flemming, H.-C. *Microbial Extracellular Polymeric Substances: Characterization, Structure and Function*; Springer Berlin Heidelberg: Berlin, Heidelberg, Germany, 1999; pp 1−19.
(5) Karatan, E.; Watnick, P. *Microbiol. Mol. Biol. Rev.* **2009**, *73*, 310−347.
(6) Flemming, H.-C.; Wingender, J. *Nat. Rev. Microbiol.* **2010**, *8*, 623−633.
(7) Waters, C. M.; Bassler, B. L. *Annu. Rev. Cell Dev. Biol.* **2005**, *21*, 319−346.
(8) von Bodman, S. B.; Willey, J. M.; Diggle, S. P. *J. Bacteriol.* **2008**, *190*, 4377−4391.
(9) Nakagami, G.; Sanada, H.; Sugama, J.; Morohoshi, T.; Ikeda, T.; Ohta, Y. *Wound Repair Regen.* **2008**, *16*, 30−36.
(10) Ron, E. Z.; Rosenberg, E. *Environ. Microbiol.* **2001**, *3*, 229−236.
(11) Allison, D. G.; Brown, M. R. W.; Evans, D. E.; Gilbert, P. *FEMS Microbiol. Lett.* **1990**, *71*, 101−104.
(12) Kearns, D. B. *Nat. Rev. Microbiol.* **2010**, *8*, 634−644.
(13) Neu, T. R. *Microbiol. Rev.* **1996**, *60*, 151−166.
(14) Miller, M. B.; Bassler, B. L. *Annu. Rev. Microbiol.* **2001**, *55*, 165−199.
(15) Lyczak, J. B.; Cannon, C. L.; Pier, G. B. *Microbes Infect.* **2000**, *2*, 1051−1060.
(16) Jarvis, F. G.; Johnson, M. J. *J. Am. Chem. Soc.* **1949**, *71*, 4124−4126.
(17) Abdel-Mawgoud, A. M.; Lépine, F.; Déziel, E. *Appl. Microbiol. Biotechnol.* **2010**, *86*, 1323−1336.
(18) Rahim, R.; Ochsner, U. A.; Olvera, C.; Graninger, M.; Messner, P.; Lam, J. S.; Soberón-Chávez, G. *Mol. Microbiol.* **2001**, *40*, 708−718.
(19) De Kievit, T. R. *Environ. Microbiol.* **2009**, *11*, 279−288.
(20) Boles, B. R.; Thoendel, M.; Singh, P. K. *Proc. Natl. Acad. Sci. U. S. A.* **2004**, *101*, 16630−16635.
(21) Déziel, E.; Comeau, Y.; Villemur, R. *J. Bacteriol.* **2001**, *183*, 1195−1204.
(22) Soberón-Chávez, G.; Lépine, F.; Déziel, E. *Appl. Microbiol. Biotechnol.* **2005**, *68*, 718−725.
(23) Zhang, J. I.; Talaty, N.; Costa, A. B.; Xia, Y.; Tao, W. A.; Bell, R.; Callahan, J. H.; Cooks, R. G. *Int. J. Mass Spectrom.* **2011**, *301*, 37−44.
(24) Hall-Stoodley, L.; Costerton, J. W.; Stoodley, P. *Nat. Rev. Microbiol.* **2004**, *2*, 95−108.
(25) Nguyen, T.; Roddick, F. A.; Fan, L. *Membranes* **2012**, *2*, 804−840.
(26) Herzberg, M.; Elimelech, M. *J. Membr. Sci.* **2007**, *295*, 11−20.
(27) Takáts, Z.; Wiseman, J. M.; Gologan, B.; Cooks, R. G. *Science* **2004**, *306*, 471−473.
(28) Watrous, J. D.; Dorrestein, P. C. *Nat. Rev. Microbiol.* **2011**, *9*, 683−694.
(29) Kerian, K. S.; Jarmusch, A. K.; Pirro, V.; Koch, M. O.; Masterson, T. A.; Cheng, L.; Cooks, R. G. *Analyst* **2015**, *140*, 1090−1098.
(30) Rao, W.; Scurr, D. J.; Burston, J.; Alexander, M. R.; Barrett, D. A. *Analyst* **2012**, *137*, 3946−3953.
(31) Meetani, M. A.; Shin, Y.-S.; Zhang, S.; Mayer, R.; Basile, F. *J. Mass Spectrom.* **2007**, *42*, 1186−1193.
(32) Badu-Tawiah, A.; Cooks, R. G. *J. Am. Soc. Mass Spectrom.* **2010**, *21*, 1423−1431.
(33) Song, Y.; Talaty, N.; Datsenko, K.; Wanner, B. L.; Cooks, R. G. *Analyst* **2009**, *134*, 838−841.
(34) Wan, J.; Meng, D.; Long, T.; Ying, R.; Ye, M.; Zhang, S.; Li, Q.; Zhou, Y.; Lin, Y. *PLoS One* **2015**, *10*, e0129978.
(35) Lanni, E. J.; Masyuko, R. N.; Driscoll, C. M.; Aerts, J. T.; Shrout, J. D.; Bohn, P. W.; Sweedler, J. V. *Anal. Chem.* **2014**, *86*, 9139−9145.
(36) Green, F. M.; Salter, T. L.; Gilmore, I. S.; Stokes, P.; O'Connor, G. *Analyst* **2010**, *135*, 731−737.
(37) Abalos, A.; Pinazo, A.; Infante, M. R.; Casals, M.; García, F.; Manresa, A. *Langmuir* **2001**, *17*, 1367−1371.
(38) Kauppila, T. J.; Talaty, N.; Salo, P. K.; Kotiaho, T.; Kostiainen, R.; Cooks, R. G. *Rapid Commun. Mass Spectrom.* **2006**, *20*, 2143−2150.
(39) Hemalatha, R. G.; Ganayee, M. A.; Pradeep, T. *Anal. Chem.* **2016**, *88*, 5710−5717.
(40) Sen, A. K.; Nayak, R.; Darabi, J.; Knapp, D. R. *Biomed. Microdevices* **2008**, *10*, 531−538.
(41) Srimany, A.; Jayashree, B.; Krishnakumar, S.; Elchuri, S.; Pradeep, T. *Rapid Commun. Mass Spectrom.* **2015**, *29*, 349−356.
(42) Sauer, K.; Camper, A. K.; Ehrlich, G. D.; Costerton, J. W.; Davies, D. G. *J. Bacteriol.* **2002**, *184*, 1140−1154.
(43) Lebron-Paler, A. *Solution and interfacial characterization of rhamnolipid biosurfactant from Pseudomonas aeruginosa ATCC 9027*, Ph.D. Dissertation, University of Arizona, Tucson, AZ, 2008.
(44) Cao, H.; Krishnan, G.; Goumnerov, B.; Tsongalis, J.; Tompkins, R.; Rahme, L. G. *Proc. Natl. Acad. Sci. U. S. A.* **2001**, *98*, 14613−14618.
(45) Madison, L. L.; Huisman, G. W. *Microbiol. Mol. Biol. Rev.* **1999**, *63*, 21−53.
(46) Davey, M. E.; Caiazza, N. C.; O'Toole, G. A. *J. Bacteriol.* **2003**, *185*, 1027−1036.

DOI: 10.1021/acs.analchem.7b04236
Anal. Chem. 2018, 90, 988−997

(47) Häußler, S.; Nimtz, M.; Domke, T.; Wray, V.; Steinmetz, I. *Infect. Immun.* **1998**, *66*, 1588−1593.
(48) Gunther, N. W.; Nuñez, A.; Fett, W.; Solaiman, D. K. Y. *Appl. Environ. Microbiol.* **2005**, *71*, 2288−2293.

DOI: 10.1021/acs.analchem.7b04236
Anal. Chem. 2018, 90, 988−997